PREDICTING WOOD CHIPS SILO DISCHARGE BEHAVIOUR - A CHOICE OF METHOD

Hamid Salehi[a], Massimo Poletto[b], Diego Barletta[b], Sylvia H. Larsson[a,*]

[a] Swedish University of Agricultural Sciences, Department of Forest Biomaterials and Technology, Biomass Technology Centre, Skogsmarksgränd, SE-90183, Umeå, Sweden
[b] Department of Industrial Engineering, University of Salerno, Via Giovanni Paolo II, 84084, Fisciano, SA, Italy

Highlights

- Silo discharge from a wedge shape silo were performed with different biomass materials.
- The ability to predict discharge behaviour by Jenike approach, Hausner ratio, angle of repose and a ring shear tester were evaluated.
- Hausner ratio showed very limited sensitivity to the biomass flow properties and was found to be very similar between different fractions.
- The best model for prediction of discharge behaviour was obtained with a square function of Angle of repose and hopper angle.

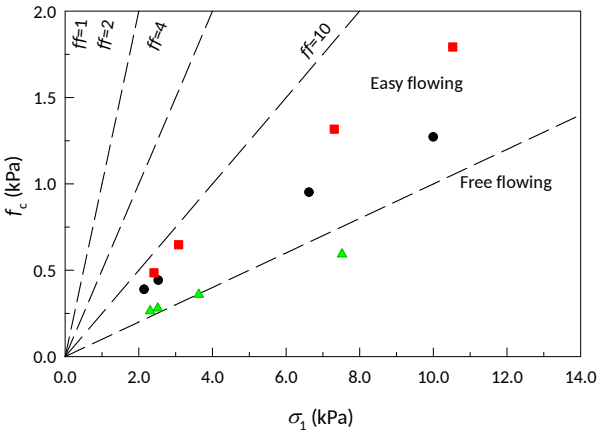
ff=1
ff=2
ff=4
ff=10
Easy flowing
Free flowing
f_c (kPa)
σ_1 (kPa)
0.0
0.5
1.0
1.5
2.0
0.0
2.0
4.0
6.0
8.0
10.0
12.0
14.0

PREDICTING WOOD CHIPS SILO DISCHARGE BEHAVIOUR - A CHOICE OF METHOD

INTRODUCTION

The interest for solid biomass fuels has been increasing over the last decades due to their potential to reduce greenhouse gas accumulation in the atmosphere and fossil fuel dependency, as well as their potential as carbon source in production of organic, chemicals or gaseous biofuels [1]. Biomass can be classified into three main groups: wood derived biomass (green waste, woody weeds, softwood, hardwood); agricultural residues (sugar cane derived, cotton derived, husk / shell, straw / stalk, oil seeds, grasses); as well as wet biomasses and organic waste (animal manure, paper sludge) [2].

The energy production from biomass has been doubled since 1989 in Sweden. In 2015, 134 TWh energy were produced from biomass of which the biggest portion, 57 TWh, were used by industries and just 13 TWh, the lowest portion, were used in transportation sector [3]. In 2014 in the European Union, the produced quantity of renewable energy was around 196 million tonnes of oil equivalents, of which 63.1 % of which was from biomass representing more than a quarter of the total primary energy produced from all sources [4]. A dramatic increase in the industrial usage of biomass, i.e. the current demand of forest biomass fuels and feedstocks for energy purposes in the petrochemical & chemical industry replacing fossil feedstock is around 30 TWh/year which is estimated to increase by 2030 to reach 45 TWh/year in Sweden [5], implies demand a robust and reliable handling of biomass bulk solids [6,7].

Storage, transfer and feeding of biomass particulate solids can be the source of a variety of flow problems [8,9]. Irregular flow of solids and blockage from storage units may occur by formation of stable arches due to both cohesion and mechanical interference between biomass particles, furthermore as a results of not isometric particle shape of biomass [10]. Bridging of biomass is documented also in thermochemical transformation units like gasification reactors [11,12]. In general, solutions to these problems involve additional equipment that, proposed on experimental bases, and are not well documented in the scientific literature. For instance, special equipment can be used to ease the silo discharge from hoppers, such as live bottom dischargers, planetary screw dischargers or air injection systems. However, adoption of these devices cause increases in handling costs and, due to the low value of biomass feedstock materials, such extra equipment costs may put at risk the economic feasibility of the whole process [11].

The arching/bridging tendencies of a variety of biomass materials through the hopper orifice of a flat bottomed container with an adjustable opening slot were experimentally determined by several researchers [13–18]. Results indicate that the critical opening size depends mainly on the particle shape, the biomass moisture content, the bed depth, the bulk density, the angle of repose, and the fraction of abnormal (hooked-shaped) and/or very long and thin particles. However, presently, in industrial applications boxes with flat bottoms are rarely used as a biomass containers. Furthermore, the relevance of the results found on experimental flat bottom containers to industrial scale silo equipped with wedge or conical shaped hoppers has not been confirmed.

Theoretical approaches was developed by Jenike [19] to predict the minimum outlet opening size to avoid arching for discharging of cohesive powders from conical and wedge shape hoppers. The Jenike approach is a function of hopper geometry, wall friction and inclination as well as material flow properties. The Jenike procedure was developed for fine, non-fibrous and rigid particulates, and it has been shown that it is not adequate to estimate the arching tendency of biomaterials with highly elastic or elongated particles, due to the limitation of standardized characterization methods for measuring flow properties of these materials [25]. The suitability of standardized powder flow properties testers, such as the Schulze shear tester, for analysis of biomass materials is strongly dependent on the size and on the shape of biomass particles [26,27].

Two faster and easier ways than shear tester analysis to assess particulate materials flowability is i) the Hausner ratio, HR, defined by the quotient between tap density and loose poured bulk density, and ii) the angle of repose, AoR, defined by the angle between the bottom surface and the sloping surface of a bulk material cone [28]. The major drawbacks of both these techniques are their empirical nature; furthermore both of them, by providing only one single index, deliver limited information on material flow properties.

Some researchers have previously used the Jenike arch stability method for determination of biomass arching behaviour. For instance, Miccio et al. [11,29,30] used a lab scale flat bottom stainless steel cylindrical vessel to study arching behaviour of different biomasses and proposed a new procedure based on Jenike arch stability approach to quantify the material flow function from the minimum opening orifice size to avoid arching.

Barletta and Poletto [6] as well as Barletta et al. [31] used a plane silo consisting of a parallelepiped bin and wedge shaped hopper to study the discharge behaviour of different biomass materials. The possibility to apply the Jenike approach [19] for calculating minimum outlet diameter to avoid

arching was evaluated for 3 different biomass materials [31]; and at different moisture content for other two different biomass materials [6]. They verified that the standard Jenike design procedure for determining minimum critical diameter to avoid arching of a wedge shape hopper is sufficiently conservative but results were randomized and no, or very poor, predictive powers can be obtained from the Jenike method for the tested biomass materials in their study Barletta et al. [6,31].

Overcoming this lack of reliable analysis methods for prediction of biomass bulk solid flow properties is something that requires research efforts and innovation. There is however a lack of basic data for finding shortcuts of where to start the development work. Such data can be used to identify which of the currently available analysis methods that gives the best predictions for biomass flow properties to, from there, continue with further development for improved predictive power.

In this study, biomass bulk solids arching behaviour was assessed utilizing a wedge-shape hopper (Figure 1) with adjustable hopper angle and outlet slot width and results were correlated to results from three different indirect flow behaviour analysis methods for determination of their predictive powers. Two different woody biomass materials were analyzed: beech stemwood and Scots pine forest residues. The two materials were chipped and fractioned into three different size assortments to form a variety in material properties and to study arch formation as a function of particle size. The three indirect analysis methods utilized for prediction of arching behaviour were 1) the standard method developed by Jenike [19] for design of a plane silo discharging, based on hopper half angle, shear cell yeild loci and wall yeild loci measurements, and the other two were 2) Hausner ratio and 3) angle of repose.

MATERIALS AND METHODS

Beech (Fagus ssp.) chips (BEC), Figure 1a, were delivered from Toulouse, France, and forest residues (FOR), Figure 1b, from north-east Sweden to the Biomass Technology Centre, Umeå, Sweden. Forest residues were dried in a plane dryer. Both assortments were shredded in a single shaft shredder (Lindner Micromat 2000, Lindner-Recyclingtech GmbH, Spittal, Austria) with a15 mm screen size. Particle size distribution of the materials was determined by sieve shaking. Materials were divided into three different fractions: $\geq$8 mm; 8$\geq$S$\geq$4 mm; and 4$\geq$S$\geq$1.9 mm, by mechanical fractioning (Mogensen E0554, Hjo, Sweden). The size distributions of the tested biomass materials before fractionation are reported in Table 1.

Silo discharge tests

Discharge experiments were carried out in a 0.3 m^3 plane silo (Figure 2) which is made by a parallelepiped bin and a wedge-shaped hopper in which it is possible to independently change both the hopper inclination angle and the width of the outlet slot. Transparent glasses on the front and the rear walls of the silo allow visual inspection of the solids inventory during flow. The other silo walls are made of stainless steel.

The silo discharge properties of each wood chip fraction was tested according to the following experimental procedure: a) adjustment of hopper angle and outlet slot width; b) bulk material loading from the silo top while the hopper opening is closed by a slab held by an hydraulic piston; c) bulk material levelling with a rake; d) very slow lowering of the closing slab which leads to either flow or arching of the material in the silo. Discharge experiments were performed at each second hopper half angle, α, from 24° to 32°, i.e. a hopper wall range steep enough to ensure mass flow conditions during discharge. For each α, the minimum outlet size to avoid stable arch formation was experimentally determined.

Angle of repose

The Geldart apparatus (Figure 3) was used to measure the angle of repose, AoR, for the tested biomass materials according to the method proposed by Geldart [32]. In this method, 500 (g) of sample are poured gently on a 45° inclinated vibrating sheet. Due to the vibration, the material is directed to a funnel, and dropped by gravity force onto a plate where a conical heap is formed. Taken heap height, h_h, and two orthogonal estimates of its base diameter, d_1 and d_2, the angle of repose, AoR, can be calculated as follows:

$$\mathrm{AoR} = \arctan\frac{4h_h}{d_1 + d_2} \tag{1}$$

Hausner ratio

The Hausner ratio is not an absolute property of the materials and its value can vary depending on the methodology used for its measurements. For instance, the ratio between tap and aerated densities is reported as a HR value in some studies [33,34] while Wong [35] used tap and poured

densities to calculate HR. In this study, tap and loose bulk density, ρ_t and ρ_b respectively, were used to calculate HR value.

$$\mathrm{HR} = \frac{\rho_t}{\rho_b} \tag{2}$$

In order to mesure the bulk density, the biomass material was poured to overfill a 50 L cylindrical container. The container has a top cpmpartment to load initially more than 50 L. Afterwards, the container was dropped from the height of 30 cm for 3 times, and overfilled again after each drop. After the third time, excess material was scraped off the top of the container without the top compartment, and finally its weight was measured. For measuring the tap density, the hight of the container was increased by mounting a cylindrical extension compartment at the top. The extended container was overfilled and vibrated with a sieve shaker for 20 minutes. After that, the upper compartment was removed, excess material was leveled off, and the weight was measured. Tap density is expected to be affected by the vibration movement and in particular by both the acceleration ratio imparted to the system and also by the frequency that indicates how often this acceleration is imparted [36,37].

INTERNAL FLOW PROPERTIES AND WALL FRICTION

A rotational Schulze ring shear tester (RST-01.01, Dietmar Schulze Schüttgutmesstechnik, Wolfenbüttel, Germany) was used to measure the internal flow properties and wall friction angles which reported in Table 3. The Schulze shear tester experimental procedure to measure materials flow properties are repoerted elswhere [27]. Assuming linear Coulomb yield loci, each yield locus was used to evaluate experimental values of the major principal stress, σ_1, and of the material unconfined yield stress, f_c. The diagram of the obtained value pairs (σ_1, f_c) provides the material flow function as reported in Figure 4.

THEORY AND HYPOTHESES OF CRITICAL ARCHING DIAMETER

In order to predict the minimum hopper slot size to avoid arching, the Jenike hopper design procedure [38], as reported also by Schulze [39], was followed. According to this approach, the arch weight is balanced by the vertical component of the abutment stress, which is the stress within the material parallel to the arch surface close to the walls. Jenike derived Equation 3 from the force balance on the arch and by assuming that the arch is unstable if the material resistance is lower than the abutment stress:

$$f_c < \frac{\rho_b g D}{h(\alpha)} \tag{3}$$

where f_c is the unconfined yield strength of the biomass, D is the effective outlet size, ρ_b is the biomass bulk density, g is the acceleration due to gravity, $h(\alpha)$ is a function which takes into account the effects of variation of the thickness of the arch with the silo geometry and the hopper half-angle, α. Schulze reported a graphical solution of measuring $h(\alpha)$ for both conical and wedge shape hopper at different hopper opening half-angle .

In mass flow silos, the consolidation stress at the outlet, σ_1, depends on the distance from the virtual hopper vertex. Making the hypothesis of radial stress field and stationary flow, Jenike derived the value of the major pincipal stress in the arch abutement, σ_1:

$$\sigma_1 = \rho_b g D \frac{(1+\sin\varphi_e)s(m,\alpha,\varphi_e,\varphi_w)}{2\sin\alpha} \tag{4}$$

where s is a complex function depending on the hopper geometry (wedge or conical), on its half angle, α, on the tensional state (m=1 for active state, m= -1 for passive state), on the biomass effective angle of internal friction and wall friction, φ_e and φ_w respectively. By combining Equations 3 and 4, it is possible to obtain the free flow criterion:

$$f_c < \sigma_1 \frac{(1+\sin\varphi_e)s(m,\alpha,\varphi_e,\varphi_w)}{h(\alpha)2\sin\alpha} = \frac{\sigma_1}{ff} \tag{5}$$

Where *ff*, as defined in the equation above, is the flow factor. The flow factor was calculated by Jenike and available in diagrams for wedge shape hoppers for different values of φ_e, where *ff* appears as a function of α, and φ_w. On the f_c - σ_1 plane, the flow factor line (σ_1/ff) cuts the flow function curve, $FF(\sigma_1)$, that is the experimental constitutive equation of the material in which the unconfined yield stress, f_c, is given as a function of the consolidation stress σ_1:

$$f_c = FF(\sigma_1) \tag{6}$$

The intersection between the flow function and the flow factor line provides the critical unconfined yield strength of the material, f_c*. The smallest outlet size, D_c, providing arch free flow, hence is given by:

$$D_c = \frac{f_c^* h(\alpha)}{\rho_b^* g} \tag{7}$$

RESULTS AND DISCUSSION

Obtained results for angle of repose, bulk and tap density and Hausner ratio for the tested materials, with standard deviations calculated from triplicate measurements, are reported in Table 2. According to Carr classification [40], an angle of repose between 40° to 50° is an indication of fairly poor flow properties while acceptable flow is found for materials which have an angle of repose below 40° and, in particular for values below 35°. It is found therefore that the beech samples, with their AoR between 36° and 50°, have poorer flow properties than the forest residue samples, whose AoR values span between 28° and 43°. Generally, the angle of repose value is attributed to factors such as the particle size, shape, surface roughness and the friction coefficient between particles. Results showed that samples with larger particles have lower AoR values and hence a higher flowability. Changes of the angle of repose with the particle size has been reported in several other studies [21,41–45].

According to the Hausner ratio (HR) flow classification, all tested biomaterials should perform as excellent flowers, particularly those with a HR lower than 1.11. In fact, an indication of poor flow behaviour is only generally considered when HR reaches values higher than 1.60 [46]. The HR values are somehow in contrast with the fairly large AoR values. HR classification was originally developed for higher density powders, which are more easily affected by the tapping procedure. For biomass materials, instead, the low density and large interparticle friction may determine a reduced effect of tapping on the final bulk density, resulting in in low Hausner ratio values. As above mentioned, the Hausner ratio shows small changes between samples, but a trend with a slight increase of the Hausner ratio with increasing particle size suggests an unlikely decrease of the material propensity to flow. The higher tap density of original particle size forest residues and a comparably higher Hausner ratio than for beech chips, might be easily explained because of the higher proportion of fine particles, including soil particles, that are able to fill the voids between larger particles and allow the attainment of larger space filling during tapping.

Table 3 reports biomaterial flow properties measured with the Schulze shear tester, namely the major principal stress, σ_1, the unconfined yield strength, f_c, material cohesion, C, the static angle of internal friction, φ_i, effective angle of internal friction, φ_e, the bulk density, ρ_b, and wall friction angle, φ_e, measured on a slide cut of the silo walls. Flow functions (the unconfined yield strength as

a function of the major principal stress during consolidation) are reported in Figure 4a for beech chips and in Figure 4b for forest residues. The unconfined yield strength is a property derived from the static yield locus through the determination of the unconfined yield Mohr circle. This parameter, therefore, is a combined function of the material cohesion, *C*, as well as the static angle of internal friction, ϕ_i. The flow functions are important because their representation is the mean by which powder flowability is usually reported and classified, according to the Jenike classification (Schulze, 2008) that is based on the flow factor value, $ff = \sigma_1/f_c$. The flow classes generally considered for powders are free-flowing (ff>10), easy flowing (4<ff≤10), cohesive (2<ff≤4), very cohesive (1<ff≤2) and hardened (ff≤1). Boundary lines between these classes and class names are reported in Figure 4. Almost all flow functions of beech wood chips, BEC, in Figure 4a fall within the easy flowing region. However, the sample with the smallest size, with particles sieved between 1.9 and 4 mm, fall on the limit between the free flowing and easy flowing ranges, attained only for the highest consolidation. Forest residue chips can also be classified as an easy flowing material. However for this material, the larger size fraction, with particles sieved between 4 to 8 mm, lies at the limit between the free and the easy flowing regions.

The working range of the Schulze shear tester is strongly dependent on the tested material particle size. Since both beech and forest residues have coarse particle sizes, it was suspected that, for some size fractions, shearing the material did not lead to the formation of a defined shear plane. This problem occurred in particular for the sieved samples with the biggest particle size, i.e. bigger than 8 mm. In fact, with these materials, it was not possible to perform shear test experiments in the attempted experiments because of the uneven position reached by the lid, as shown in Figure 5. Shearing these kinds of materials leads to a redistribution of their particles in the lid pockets instead of shearing the materials and, hence, causing a raising lid and void formation at the pocket back. This problematic issue was also observed and illustrated in more details by Barletta et al. [31].

Obtained results from the silo discharge experiments are shown in Table 1 in appendix and Figure 6, displaying the required slot opening size, *D*c, to avoid arching, reported as a function of the hopper half angle, α, for all particle size fractions of the tested biomaterials. In general, the value of D_c increased by increasing the hopper half angle. Furthermore, the critical outlet opening to avoid arching was largest for the finest fractions. The finest sieved fractions had the smallest critical outlet opening size and the D_c for whole particle range materials fell in between the two. Critical outlet sizes of beech chip samples were larger than for the forest residues in all size fractions. These differences do not completely correspond to the classification of flow properties of materials

derived from flow function tests (Figure 4). This is however not surprising since also the bulk density is important in the determination of the critical slot width. For beech wood chips, the experimental D_c values for >8 mm samples were very close to the values for 4 to 8 mm samples (Figure 6a). In spite of the fairly different flow functions, the same was true for the non-fractioned and 4 to 8 mm forest residue samples (Figure 6b).

According to the design theory presented above, the flow properties reported in Table 3 are used to evaluate design values reported in Table 1 in appendix and Figure 6. Namely, values of $h(\alpha)$ functions at different hopper half angle were evaluated based on the method developed by Schulze [39] and values of flow factor, ff , from the Jenike diagrams reported by Schulze [39]. The intersection between the ff line and the flow functions and density curves measured by the Schulze shear tester determined the critical values of the unconfined yield strength, f_c^*, as well as critical value of bulk density, ρ_b^*. These values were used in Equation 8 to calculate the prediction values of the critical slot opening to avoid arching based on the Jenike approach. As above mentioned, it was not possible to measure flow properties of both biomass samples with particle size larger than 8 mm and, therefore design values for these materials are not reported in Figure 6 and Table 1 in appendix.

Design values for the critical slot width confirm all experimental trends found with the hopper half angle and the particle size distribution of the samples. Nevertheless, comparing experimental and design results, clearly shows that the predicted critical hopper outlet size for both tested materials and all size fractions are sufficiently conservative and its value is higher than the critical hopper outlet experimental values for all the size fractions and at the fixed value of α. This difference between experimental and predicted values might be due to the limited validity for biomass materials in the arch formation and breakage analysis by Jenike. For example, arch stability for fibrous biomaterial could be attributed to the tensile strength of the material instead of unconfined yield strength [31]. In fact, for these kinds of materials cohesion might not be the predominant mechanism to stabilize an arch, where the material instead might be connected to the upper layer inside the silo by the effect of bulk tensile strength.

Figure 6a shows that Jenike design values vs. experimental values found for D_c. It has to be recalled that the Jenike procedure is a silo design procedure which tends to provide silo design estimates on the safe side, therefore the comparison with the experimental values on a parity plot may not be approriate and, in fact, as above mentioned, all Jenike predictions are higher than the experimental values. However, in order to understand if the procedure is able to correctly account for the the

differences in the flow behaviour found for the tested biomass materials, Figure 7a reports also the values of the Jenike prediction reduced by a factor of 0.722. This factor was obtained as the coefficent which minimize the sum of quadratic differences between the experimental values of D_c and the Jenike prediction, which therefore represent the average design safety factor of the Jenike prediction. The low value of $R^2 = 0.36$, suggests an inadequacy of the Jenke procedure to correctly account for difference in the flow behaviour of the tested biomass materials.

Considering the other tested flow properties it was observed a qualitative good correlation between the flow behaviour of powders and the angle of repose, AoR. In order to verify if it is possible to correlate the experimental critical hopper opening for both materials and the angle of repose as well as with the hopper angle, different possible equations was tested with a regression procedure. The one which has produced the better results is the following:

$$D_c = a * AoR^b * \alpha^c \tag{8}$$

Table 4 reports the best fitting values of the parameters *a*, *b*, and *c*, that minimize the sum of squared errors. The same table also reports the *p*-values for the regressed parameters with a significance level of 0.05% and the 95% confidence intervals of the same parameters. The low *p*-values support the compatibility between our data and the regression model proposed, which is also supported by the value of the determination coefficient $R^2 = 0.78$. This finding indicates a better performance of Equation (8) with the regression values of Table 4 also with respect of the Jenike prediction reduced for the estimated average design safety factor. Figure 7b reports the comparison between the predicted values of D_c provided by Equation (8) with the regression values of Table 4. It is noteworthy that the two materials seems to be equally well fitted by the same equation and that for the sets of data studied the correlation of D_c with the AoR and α seems not to be affected by the kind of material analyzed. Furthermore, the possibility to relate the AoR with D_c suggests that the main material properties that produce the angle in a pile (friction, cohesion and gravity) act with mechanisms with similar relative importance in the silo discharge experiment.

CONCLUSIONS

Flow property measurements as well as angle of repose, tap and bulk densities of beech chips and forest residue with different size fractions were performed. Furthermore, several silo discharge tests of the both materials have been carried out at different hopper half angle and opening width to find out the critical opening size that leads to the formation of stable arch.

The Hausner ratio did not show to be significantly affected for the different biomass, hence not a significant parameter to predict the biomass propensity to flow. A possible reason might be the high interparticle friction and the low density of the biomass materials. As expected for material of different bulk density, also the biomass shear testing did not correlate directly with the biomass propensity to flow in terms of critical opening size.

A much better correlation with the silo experimental critical opening was provided by using the Jenike approach. However this method, provided design values of the critical opening size that were largely on the safe side, considering hopper design objectives, than the experimental values. An average safety factor was calculated to be around 0.7.

The measured biomass property which seemed to better correlate with the critical opening size was the angle of repose. This finding may suggest that the main material properties that produce the angle in a pile (friction, cohesion and gravity) act with mechanisms with similar relative importance in the silo discharge experiment. An empirical single fitting equation for the two materials was proposed to relate the critical opening size with the angle of repose and the hopper half opening angle. It turns out that the critical opening size of the hopper is linearly proportional to the hopper half opening angle and to the square of the angle of repose.

ACKNOWLEDGEMENTS

The authors wish to thank the Swedish Energy Agency for providing a grant for this research project.

Raw materials were received from the MOBILE FLIP project which has received funding from the European Union's Horizon 2020 research and innovation programme under grant agreement number 637020−MOBILE FLIP.

NOMENCLATURE

AoR angle of repose, deg.

C cohesion, Pa

D effective outlet size, m

d_1 major base diameter of the heap, m

d_2 base diameter of the heap orthogonal to the major, m

D_c critical outlet size, m

f_c unconfined yield strength, Pa

f_c^* critical unconfined yield strength, Pa

ff flow factor, -

FF flow function, -

g the acceleration due to gravity, m.s

HR Hausner ratio, -

h function which takes into account effects of variation of thickness of the arch with the silo geometry and the hopper half-angle α, -

h_h heap height for calculating AoR, m

S a function depending on hopper geometry, on half angle, α, on the tensional state (*m* = 1 for active state, *m* = -1 for passive state), on effective angle of internal friction, ϕ_e, and on wall friction, ϕ_w, -

Greek symbols

α hopper half angle, deg.

φ_i kinematic angle of internal friction, deg.

φ_e effective angle of internal friction, deg.

ϕ_w angle wall friction, deg.

σ_1 major principal stress, Pa

ρ_b bulk density, kg.m^{-3}

ρ_{b*} critical bulk density, kg.m^{-3}

ρ_t tap density, $kg.m^{-3}$

REFERENCES

[1] A. Giuliano, R. Cerulli, M. Poletto, G. Raiconi, D. Barletta, Process Pathways Optimization for a Lignocellulosic Biorefinery Producing Levulinic Acid, Succinic Acid, and Ethanol, Ind. Eng. Chem. Res. (2016) acs.iecr.6b01454. doi:10.1021/acs.iecr.6b01454.

[2] D. Barletta, M. Poletto, An Assessment on Silo Design Procedures for Granular Woody Biomass, (n.d.). http://www.aidic.it/cet/13/32/369.pdf (accessed April 5, 2017).

[3] Publications, The Swedish Energy Agency. (2017). http://www.energimyndigheten.se/en/facts-and-figures/publications/ (accessed December 4, 2017).

[4] C. Calderón, G. Gauthier, J.-M. Jossart, P. Archambeau, F.-P. Langue, N. Hemeleers, A. Aveni, J.-B. Boucher, AEBIOM Statistical Report, 2016. www.aebiom.org (accessed September 18, 2017).

[5] P. Börjesson, J. Hansson, G. Berndes, Future demand for forest-based biomass for energy purposes in Sweden, For. Ecol. Manage. 383 (2017) 17–26. doi:10.1016/j.foreco.2016.09.018.

[6] D. Barletta, M. Poletto, An assessment on silo design procedures for granular woody biomass, 2013. doi:10.3303/CET1332369.

[7] T.A. Lestander, B. Johnsson, M. Grothage, NIR techniques create added values for the pellet and biofuel industry, Bioresour. Technol. 100 (2009) 1589–1594. doi:10.1016/j.biortech.2008.08.001.

[8] A. Owonikoko, R.J. Berry, M.S.A. Bradley, The difficulties of handling biomass and waste: Characterisation of extreme shape materials, Bulk Solids Handl. 31 (2011).

[9] Á. Ramírez-Gómez, Research needs on biomass characterization to prevent handling problems and hazards in industry, Part. Sci. Technol. 34 (2016) 432–441. doi:10.1080/02726351.2016.1138262.

[10] Z. Guo, X. Chen, H. Liu, H. Chen, Gravity discharge characteristics of biomass-coal blends in a hopper, Fuel. 125 (2014) 137–143. doi:10.1016/j.fuel.2014.02.009.

[11] F. Miccio, D. Barletta, M. Poletto, Flow properties and arching behavior of biomass particulate solids, Powder Technol. 235 (2013) 312–321. doi:10.1016/j.powtec.2012.10.047.

[12] J. Dai, H. Cui, J.R. Grace, Biomass feeding for thermochemical reactors, Prog. Energy Combust. Sci. 38 (2012) 716–736. doi:10.1016/J.PECS.2012.04.002.

[13] J.E. Mattsson, Basic handling characteristics of wood fuels: Angle of repose, friction against surfaces and tendency to bridge for different assortments, Scand. J. For. Res. 5 (1990) 583–597. doi:10.1080/02827589009382641.

[14] J.E. Mattsson, Tendency to bridge over openings for chopped Phalaris and straw of Triticum mixed in different proportions with wood chips, Biomass and Bioenergy. 12 (1997) 199–210. doi:10.1016/S0961-9534(96)00048-7.

[15] J.E. Mattsson, P.D. Kofman, Method and apparatus for measuring the tendency of solid biofuels to bridge over openings, Biomass and Bioenergy. 22 (2002) 179–185. doi:10.1016/S0961-9534(01)00067-8.

[16] J.E. Mattsson, P.D. Kofman, Influence of particle size and moisture content on tendency to bridge in biofuels made from willow shoots, Biomass and Bioenergy. 24 (2003) 429–435. doi:10.1016/S0961-9534(02)00178-2.

[17] P.D. Jensen, J.E. Mattsson, P.D. Kofman, A. Klausner, Tendency of wood fuels from whole trees, logging residues and roundwood to bridge over openings, Biomass and Bioenergy. 26 (2004) 107–113. doi:10.1016/S0961-9534(03)00101-6.

[18] S. Hinterreiter, H. Hartmann, P. Turowski, Method for determining bridging properties of biomass fuels-experimental and model approach, Biomass Convers. Biorefinery. 2 (2012) 109–121. doi:10.1007/s13399-012-0033-7.

[19] A.W. Jenike, Gravity flow of solids, Trans Instn Chem Engrs. 40 (1962) 264.

[20] J.M. Craven, J. Swithenbank, V.N. Sharifi, Investigation into the Flow Properties of Coarse Solid Fuels for Use in Industrial Feed Systems, J. Powder Technol. 2015 (2015) 1–12. doi:10.1155/2015/786063.

[21] Z. Guo, X. Chen, Y. Xu, H. Liu, Study of flow characteristics of biomass and biomass–coal blends, Fuel. 141 (2015) 207–213. doi:10.1016/j.fuel.2014.10.062.

[22] M. Zulfiqar, B. Moghtaderi, T.F. Wall, Flow properties of biomass and coal blends, Fuel Process. Technol. 87 (2006) 281–288. doi:10.1016/j.fuproc.2004.10.007.

[23] D. Barletta, A. Diaz, L. Esposito, L. Montenegro, J.M. Sanchez, M. Poletto, Characterisation of Flow Properties of Coal-Petcoke-Biomass Mixtures for Co-firing, (n.d.). http://www.aidic.it/cet/13/32/255.pdf (accessed April 5, 2017).

[24] P. Chen, Z. Yuan, X. Shen, Y. Zhang, Flow properties of three fuel powders, Particuology. 10 (2012) 438–443. doi:10.1016/j.partic.2011.11.013.

[25] M. Gil, D. Schott, I. Arauzo, E. Teruel, Handling behavior of two milled biomass: SRF poplar and corn stover, Fuel Process. Technol. 112 (2013) 76–85. doi:10.1016/j.fuproc.2013.02.024.

[26] F. Miccio, A. Landi, D. Barletta, M. Poletto, Preliminary assessment of a simple method for evaluating the flow properties of solid recovered fuels, Part. Sci. Technol. 27 (2009). doi:10.1080/02726350902775988.

[27] H. Salehi, D. Barletta, M. Poletto, A comparison between powder flow property testers, Particuology. 32 (2017) 10–20. doi:10.1016/j.partic.2016.08.003.

[28] M.R. Wu, D.L. Schott, G. Lodewijks, Physical properties of solid biomass, (2011). doi:10.1016/j.biombioe.2011.02.020.

[29] F. Miccio, N. Silvestri, D. Barletta, M. Poletto, Characterization of woody biomass flowability, Chem. Eng. Trans. 24 (2011) 643–648. doi:10.3303/CET1124108.

[30] F. Miccio, A. Landi, D. Barletta, M. Poletto, Preliminary Assessment of a Simple Method for Evaluating the Flow Properties of Solid Recovered Fuels, http://dx.doi.org/10.1080/02726350902775988. (2009). doi:10.1080/02726350902775988.

[31] D. Barletta, R.J. Berry, S.H. Larsson, T.A. Lestander, M. Poletto, Á. Ramírez-Gómez, Assessment on bulk solids best practice techniques for flow characterization and storage/handling equipment design for biomass materials of different classes, Fuel Process. Technol. 138 (2015) 540–554. doi:10.1016/j.fuproc.2015.06.034.

[32] D. Geldart, E.C. Abdullah, A. Hassanpour, L.C. Nwoke, I. Wouters, Characterization of powder flowability using measurement of angle of repose, China Particuology. 4 (2006)

104–107. doi:10.1016/S1672-2515(07)60247-4.

[33] N. Harnby, A.E. Hawkins, D. Vandame, The use of bulk density determination as a means of typifying the flow characteristics of loosely compacted powders under conditions of variable relative humidity, Chem. Eng. Sci. 42 (1987) 2067. doi:10.1016/0009-2509(87)80156-2.

[34] E.C. Abdullah, D. Geldart, The use of bulk density measurements as flowability indicators, Powder Technol. 102 (1999) 151–165. doi:10.1016/S0032-5910(98)00208-3.

[35] A. Chi-Ying Wong, Characterisation of the flowability of glass beads by bulk densities ratio, Chem. Eng. Sci. 55 (2000) 3855–3859. doi:10.1016/S0009-2509(00)00048-8.

[36] A. Santomaso, P. Lazzaro, P. Canu, Powder flowability and density ratios: the impact of granules packing, Chem. Eng. Sci. 58 (2003) 2857–2874. doi:10.1016/S0009-2509(03)00137-4.

[37] H. Salehi, N. Lotrecchiano, D. Barletta, M. Poletto, Dust Release from Aggregative Cohesive Powders Subjected to Vibration, Ind. Eng. Chem. Res. 56 (2017) 12326–12336. doi:10.1021/acs.iecr.7b02241.

[38] A. Jenike, Storage and flow of solids, Bull. Univ. Utah. (1964). https://www.osti.gov/scitech/servlets/purl/5240257 (accessed May 15, 2017).

[39] D. Schulze, Powders and Bulk Solids, Springer Berlin Heidelberg, Berlin, Heidelberg, 2008. doi:10.1007/978-3-540-73768-1.

[40] Y.S.L. Lee, R. Poynter, F. Podczeck, J.M. Newton, Development of a dual approach to assess powder flow from avalanching behavior, AAPS PharmSciTech. 1 (2000) 44–52. doi:10.1208/pt010321.

[41] M.A. CARRIGY, EXPERIMENTS ON THE ANGLES OF REPOSE OF GRANULAR MATERIALS1, Sedimentology. 14 (1970) 147–158. doi:10.1111/j.1365-3091.1970.tb00189.x.

[42] J.T. Carstensen, P.C. Chan, Relation between particle size and repose angles of powders, Powder Technol. 15 (1976) 129–131. doi:10.1016/0032-5910(76)80037-X.

[43] R.L. Stewart, J. Bridgwater, Y.C. Zhou, A.B. Yu, Simulated and measured flow of granules

in a bladed mixer—a detailed comparison, Chem. Eng. Sci. 56 (2001) 5457–5471. doi:10.1016/S0009-2509(01)00190-7.

[44] Y.C. Zhou, B.H. Xu, A.B. Yu, P. Zulli, An experimental and numerical study of the angle of repose of coarse spheres, Powder Technol. 125 (2002) 45–54. doi:10.1016/S0032-5910(01)00520-4.

[45] Z. Miao, T.E. Grift, A.C. Hansen, K.C. Ting, Flow performance of ground biomass in a commercial auger, Powder Technol. 267 (2014) 354–361. doi:10.1016/j.powtec.2014.07.038.

[46] R.B. Shah, M.A. Tawakkul, M.A. Khan, Comparative evaluation of flow for pharmaceutical powders and granules., AAPS PharmSciTech. 9 (2008) 250–8. doi:10.1208/s12249-008-9046-8.

Figure 1. a) Beech chips (BEC); b) forest residues (FOR)

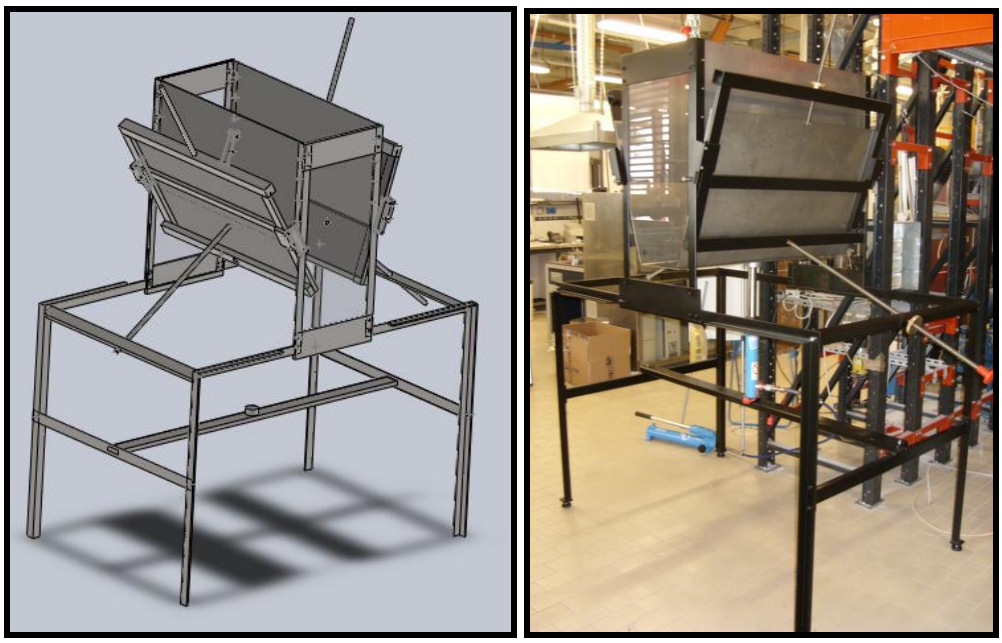

Figure 2. Wedge-shaped hopper used for silo discharge tests

Figure 3. The Geldart apparatus to measure angle of repose [32]

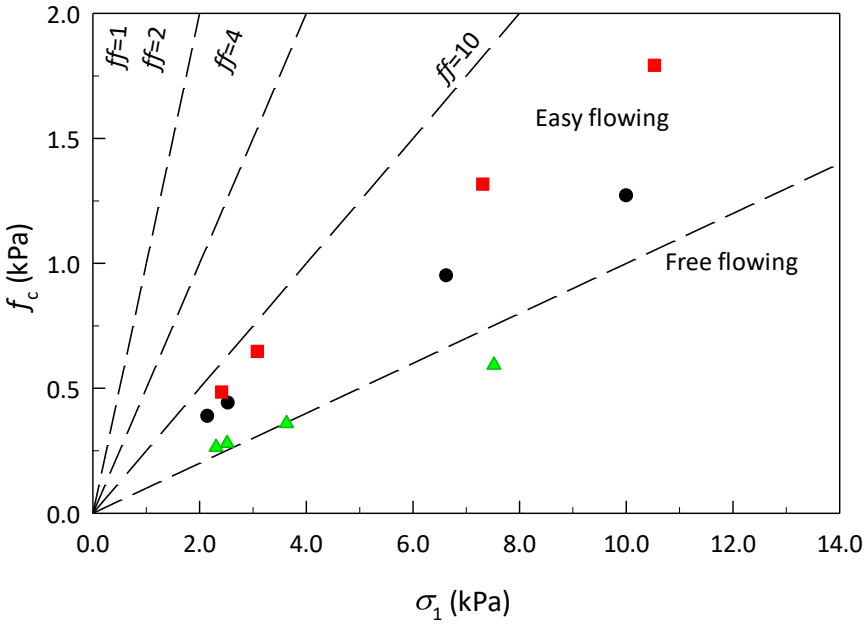

a)

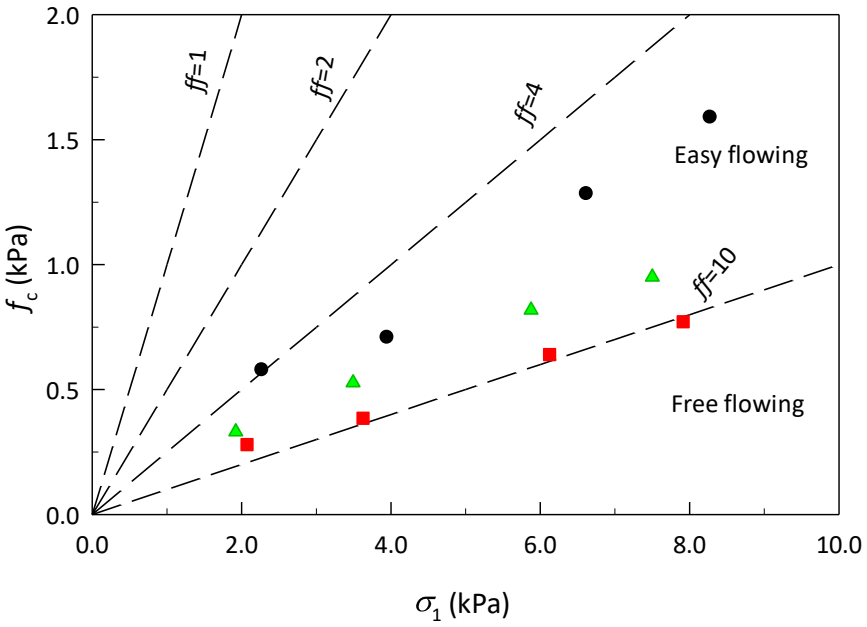

b)

Figure 4. Biomass flow properties of a) beech and b) forest residue chips at different size fractions of ▲,1.9 - 4.0 mm; ■, 4.0 – 8.0 mm; and ●, the whole particle range.

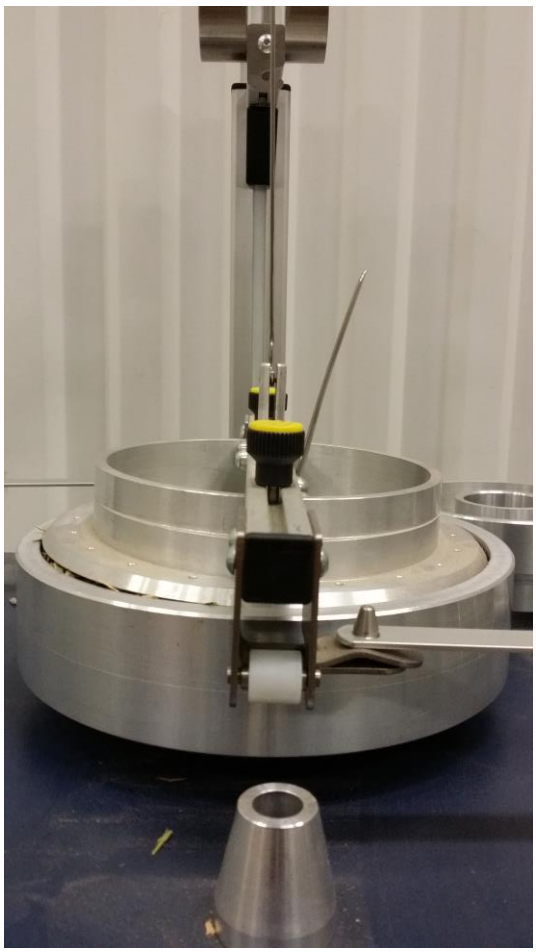

Figure 5. Uneven position of the Schulze shear tester lid during shear testing of large particle size materials.

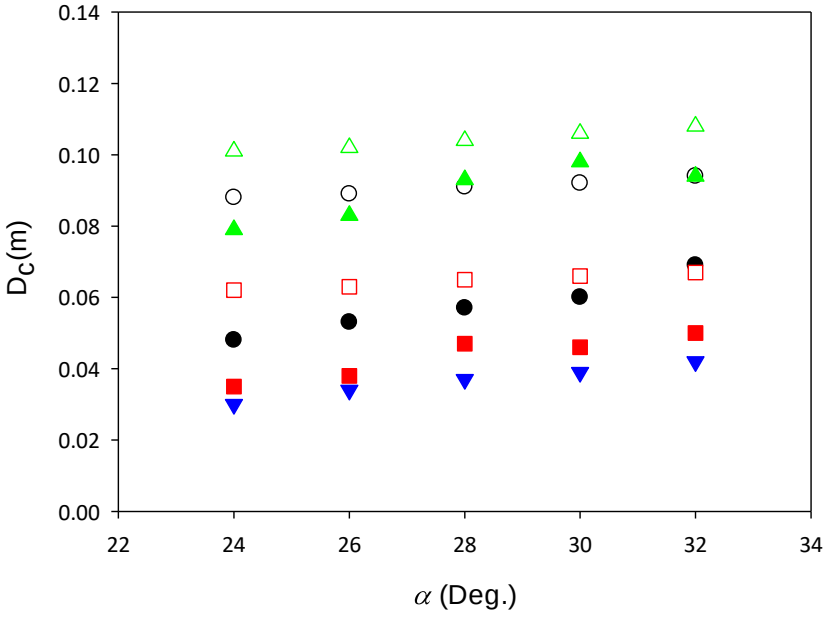

a)

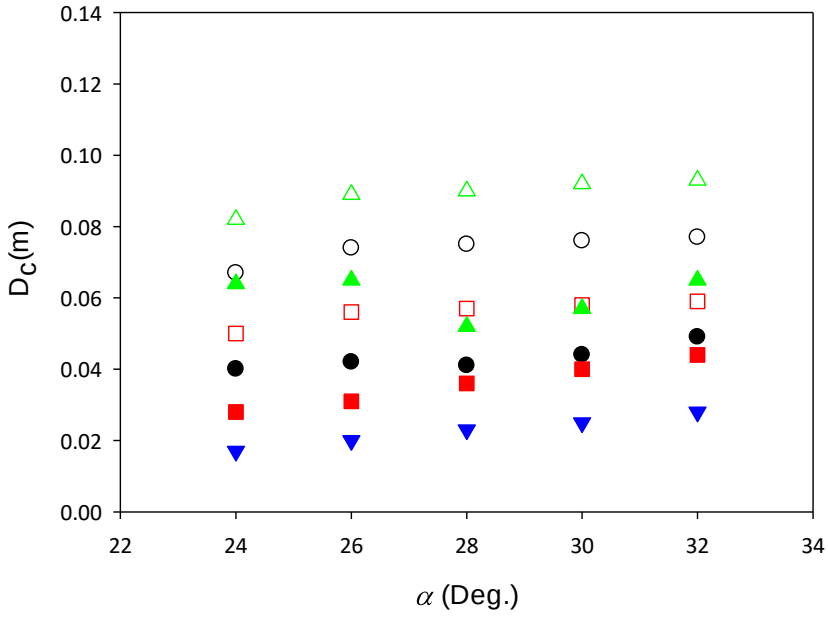

b)

Figure 6. Critical hopper outlet size to avoid arching for a) beech and b) forest residue chips of different size fractions; ▲, 1.9 – 4.0 mm experimental results; △, 1.9 – 4.0 mm modelling results; ■, 4.0 – 8.0 mm experimental results; ◻, 4.0 – 8.0 mm modelling results; ●, whole material experimental results; ⭘; whole material experimental results; ▼, ≥ 8.0 mm experimental results.

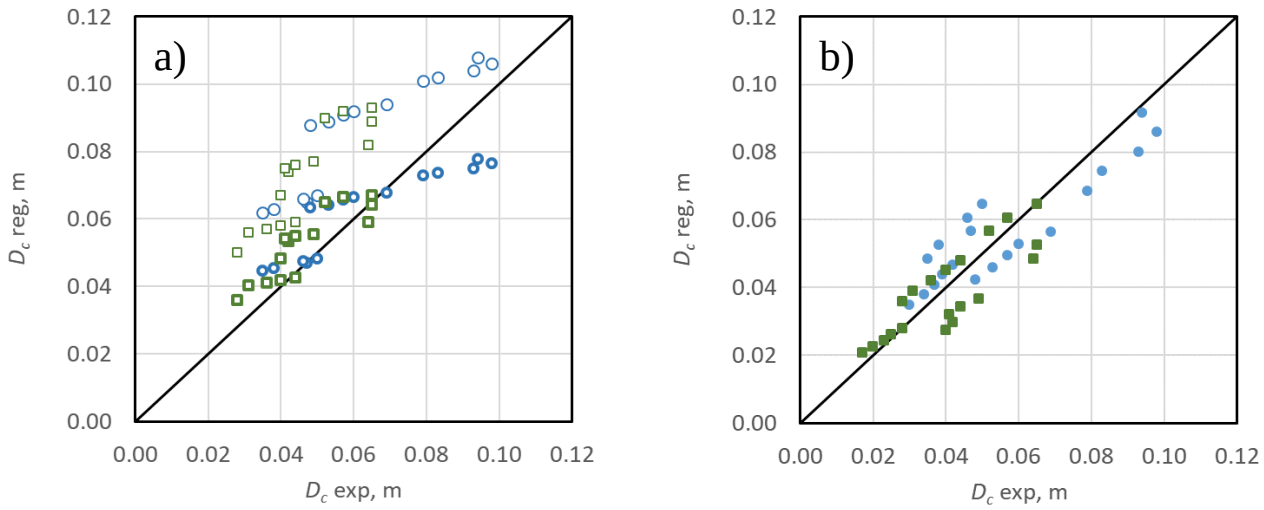

Figure 7. Comparison within model estimates of the critical hopper outlet size vs the experimental values. a) *J*enike design estimates: ○, BEC; □; forest residue; ◎, BEC with 0.722 reduction; ▣; forest residue with 0.722 reduction. b) Equation (8) with the best fitting parameters of Table 4: ●, BEC; ■; forest residue.

Table 1. Size fractions of the tested biomass materials

	>8.0 mm (%)	4.0-8.0 mm (%)	1.9-4.0 mm (%)	1.0-1.9 mm (%)	0.5-1.0 mm (%)
BEC	40.5	34.4	14.6	5.2	3.1
Forest residue	20.4	27.3	26.1	12.7	6.8

Table 2. Flow indexes of the different biomass fractions

Size fraction (mm)	AoR (Deg)	ρ_b (kg m^{-3})	ρ_t (kg m^{-3})	H (-)
		BEC		
whole	40.3±0.5	250±1.4	294±0.7	1.17
≥ 8. 0 mm	36.7±0.2	222±1.9	268±0.8	1.20
4.0 - 8.0 mm	43.1±0.7	250±0.5	280±2.7	1.12
1.9 - 4.0 mm	51.2±1.4	295±1.8	318±0.6	1.07
		Forest residue		
Not fractioned	32.5±0.7	227±2.6	314±2.4	1.38
≥ 8.0 mm	28.4±0.5	268±1.8	315±1.3	1.17
4.0 - 8.0 mm	37.2±0.8	262±0.9	297±0.7	1.13
1.9 - 4.0 mm	43.1±0.6	327±1.5	340±2.5	1.04

Table 3. Flow properties of the biomass particulate materials

Size fraction (mm)	σ_1 (Pa)	f_c (Pa)	C (Pa)	φ_i (Deg)	φ_e (Deg)	ρ_b (kg m^{-3})	φ_w (Deg)
			Beech chips				
whole particle	2150	387	37	40.9	38	242	23
range	2534	440	45	42.1	36.4	259	
	6627	950	218	48.6	45.2	274	
	10006	1270	286	47.6	44.9	309	
4.0 - 8.0 mm	2410	485	45	43.5	48.9	269	
	3080	647	61	44.0	48.6	270	23
	7307	1317	269	46.3	48.2	208	
	10527	1793	448	44.5	45.9	262	
1.9 - 4.0 mm	2306	264	42	46.7	50.8	140	
	2515	280	63	45.4	48.0	160	21
	3630	359	68	45.4	50.4	168	
	7519	593	82	46.3	51.5	173	
			Forest residue chips				
whole particle	2268	579	137	44.5	46.5	204	16
range	3945	709	145	43.7	49.3	192	
	6616	1284	309	41.2	48.0	192	
	8275	1590	347	40.2	49.8	205	
4.0 - 8.0 mm	2071	280	70	42.0	47.3	200	19
	3625	385	81	42.0	49.3	202	
	6125	640	172	40.2	42.9	199	
	7914	772	244	39.4	44.3	213	
1.9 - 4.0 mm	1922	331	65	41.6	45.4	170	17
	3491	527	101	40.0	45.5	166	
	5878	819	151	41.0	43.1	151	
	7501	951	229	36.4	39.3	158	

Table 4. Best fitting regression parameters of Equation (8).

Parameter	Best fit value	*p*-value	95% confidence interval	
			Lower limit	Upper limit
a	$9.55 \cdot 10^{-7}$	$3.48 \cdot 10^{-13}$	$7.84 \cdot 10^{-8}$	$1.66 \cdot 10^{-5}$
b	2.03	$1.75 \cdot 10^{-13}$	1.65	2.40
c	1.01	$2.45 \cdot 10^{-3}$	0.380	1.64

Appendix

Table1. Arching behaviour of biomass particulate materials

Size fraction (mm)	α (Deg)	h (-)	ff (-)	f_c^* (Pa)	ρ_b^* (kg m^3)	D_c (Mo) (m)	D_c (Ex) (m)
Beech wood chips							
whole	24	1.09	1.20	194.1	154.3	0.088	0.048
	26	1.10	1.20	194.1	154.3	0.089	0.053
	28	1.12	1.20	194.1	154.3	0.091	0.057
	30	1.14	1.20	194.1	154.3	0.092	0.060
	32	1.16	1.20	194.1	154.3	0.094	0.069
≥ 8.0 mm	24	-	-	-	-	-	0.030
	26	-	-	-	-	-	0.034
	28	-	-	-	-	-	0.037
	30	-	-	-	-	-	0.039
	32	-	-	-	-	-	0.042
4.0 - 8.0 mm	24	1.09	1.20	224.8	127.0	0.062	0.035
	26	1.10	1.20	224.8	127.0	0.063	0.038
	28	1.12	1.20	224.8	127.0	0.065	0.047
	30	1.14	1.20	224.8	127.0	0.066	0.046
	32	1.16	1.20	224.8	127.0	0.067	0.050
1.9 - 4.0 mm	24	1.09	1.20	108.9	119.4	0.101	0.079
	26	1.10	1.20	108.9	119.4	0.102	0.083
	28	1.12	1.20	108.9	119.4	0.104	0.093
	30	1.14	1.20	108.9	119.4	0.106	0.098
	32	1.16	1.20	108.9	119.4	0.108	0.094
Forest residue chips							
Not fractioned	24	1.10	1.19	110.3	166.0	0.067	0.040
	26	1.10	1.20	109.2	164.6	0.074	0.042
	28	1.12	1.22	107.1	161.9	0.075	0.041
	30	1.14	1.25	104.1	158.0	0.076	0.044
	32	1.16	1.26	103.2	156.8	0.077	0.049
≥ 8.0 mm	24	-	-	-	-	-	0.017
	26	-	-	-	-	-	0.020
	28	-	-	-	-	-	0.023
	30	-	-	-	-	-	0.025
	32	-	-	-	-	-	0.028

Size fraction (mm)	α (Deg)	h (-)	ff (-)	f_c^* (Pa)	ρ_b^* (kg m^3)	D_c (Mo) (m)	D_c (Ex) (m)
4.0 - 8.0 mm	24	1.10	1.36	70.8	139.8	0.050	0.028
	28	1.12	1.39	69.2	136.8	0.057	0.036
	30	1.14	1.41	68.1	134.9	0.058	0.040
	32	1.16	1.43	67.1	133.0	0.059	0.044
1.9 - 4.0 mm	24	1.0	1.38	100.2	126.1	0.082	0.064
	26	1.1	1.40	98.7	124.3	0.089	0.065
	28	1.12	1.41	97.9	123.4	0.090	0.052
	30	1.14	1.43	96.4	121.7	0.092	0.057
	32	1.16	1.45	95.0	120.0	0.093	0.065